PHYSICAL REVIEW C VOLUME 15, NUMBER 2 FEBRUARY 1977

# Neutron total cross sections and resonance parameters of $^{63}_{29}$Cu and $^{65}_{29}$Cu. I*

M. S. Pandey† and J. B. Garg‡
*State University of New York at Albany, Albany, New York 12222*

J. A. Harvey
*Oak Ridge National Laboratory, Oak Ridge, Tennessee 37830*
(Received 8 April 1976)

High resolution neutron total cross sections of the isotopes of copper have been measured from about 10 to 150 keV using 5 nsec electron pulses and a flight path of 78.2 m. From the area and shape analysis of the transmission and total cross section data, precise values of the resonance parameters, such as $E_0$, $\Gamma_n^0$, $\Gamma_n^1$, $J^\pi$, etc., have been determined. For example, for $^{63}$Cu many $s$-wave resonances have been observed from 10 to 150 keV giving values of $\langle D\rangle_{J=1} = (2.7 \pm 0.3)$ keV, $\langle D\rangle_{J=2} = (4.0 \pm 0.5)$ keV, $\langle D\rangle_{J=1+2} = (1.63 \pm 0.13)$ keV, $S_{0\,J=1} = (3.0 \pm 0.6) \times 10^{-4}$ eV$^{-1/2}$, $S_{0\,J=2} = (2.0 \pm 0.5) \times 10^{-4}$ eV$^{-1/2}$, $S_{0\,J=1,2} = (2.5 \pm 0.4) \times 10^{-4}$ eV$^{-1/2}$. For $^{65}$Cu $s$-wave resonances were observed giving values of $\langle D\rangle_{J=1} = (3.6 \pm 0.4)$ keV, $\langle D\rangle_{J=2} = (5.0 \pm 0.7)$ keV, $\langle D\rangle_{J=1+2} = (2.12 \pm 0.19)$ keV, $S_{0\,J=1} = (2.9 \pm 0.6) \times 10^{-4}$ eV$^{-1/2}$, $S_{0\,J=2} = (1.8 \pm 0.5) \times 10^{-4}$ eV$^{-1/2}$, $S_{0\,J=1,2} = (2.3 \pm 0.4) \times 10^{-4}$ eV$^{-1/2}$.

[NUCLEAR REACTIONS $^{63,65}$Cu$(n,n)$, deduced $E_0$, $\Gamma_n$, $S_0$, $\langle D\rangle$, etc., and investigated the distribution about their average values.]

## I. INTRODUCTION

Precise measurements of neutron total cross sections of nuclei provide valuable information for the investigation of neutron interactions with nuclei. The systematics of strength function, level densities, etc., and their dependence upon resonance parameters such as spin and parity are important. These measurements of certain nuclei are also important for their application in reactor design. The measurements of the separated isotopes of copper were undertaken for these considerations and the fact that the Oak Ridge Electron Linear Accelerator (ORELA) neutron facility has the highest resolution for making such measurements up to a few hundred keV neutron energy.

## II. EXPERIMENTAL FACILITY

These measurements were made at the ORELA; which has been built primarily for accurate, high resolution neutron cross section data. The accelerator was operated at a nominal energy of about 150 MeV with electron bursts width of 5 nsec and a repetition rate of 1000 pulses/sec.

Neutrons are produced with a peak intensity of $\sim 6 \times 10^{18}$ neutrons/sec in a small water-cooled laminated Ta target capable of dissipating about 60 kW of power. The evaporation neutrons from the Ta, with an average energy of ~1 MeV, are moderated by the 3 cm thick, 15 cm diameter $C$-shaped water moderator around the target. The disk radius of 7.5 cm ($H_2O$) yielded 90% of the infinite intensity, calculated from a point isotropic source of 1-MeV neutrons at the center of the target. The neutron spectrum from the moderator varies approximately as $E_n^{-0.82}$. This corresponds to an average leakage probability per collision in the moderator of ~8%. The fraction of neutrons reaching thermal energies in the moderator is estimated to be $3 \times 10^{-4}$ and ~12% of these will be captured by the hydrogen of the water moderator and produce 2.23-MeV $\gamma$ rays.

### Neutron detectors

The neutron detectors are shielded from direct $\gamma$ flash from the Ta target by a shadow bar. The collimators are selected so that the detectors only "see" the water moderator. A few mm of a Pb filter in the beam reduces the $\gamma$ flash from the water moderator by an order of magnitude. The moderated neutrons travel down a flight path with detector stations located at 80 and 200 m from the target. The characteristics of the accelerator (pulse width, repetition rate, etc.), are chosen to optimize measurements in the neutron energy region from 3 to 500 keV. Below ~5 keV the energy resolution is determined by the uncertainty of the length of the neutron flight path due to the neutron source and the finite size of the detector, while above ~500 keV the resolution is mainly governed by the neutron burst width. Typical values of the energy resolution ($\Delta E/E$) range from 0.003 to 0.0005, depending on the experiment, which dictates the flight distance, electron beam pulse width, and neutron energy.

The data acquisition system of the ORELA consists of three computers, each capable of handling four simultaneous experiments.[1] The system provides hundreds of thousands of channels, too many to be provided by direct-core memory, and yet operates at count rates (up to 5000 events/sec) which are too high to permit the use of a magnetic tape system. The system updates totalized data on a magnetic disk. The computers are capable of performing preliminary operations and periodic checks on the data in addition to carrying out the updating function. As an example, one can vary channel widths as a function of neutron energy in order to minimize the number of channels required in an experiment and avoid recording the purely background information. One can also display selected portions of data and carry out the usual operation of listing and plotting the data.

The present measurements were made at a flight distance of 78.2 m and time-of-flight analyzer channel widths varying from 1 nsec at short times to larger widths at long flight times. The nominal resolution of the measurements corresponds to 0.05 nsec/m at the highest energy.

The neutron flight path is evacuated during the experiment. The two samples of $^{63,65}$Cu isotopes in separate sample holders are inserted in the beam and are cycled in and out of the beam by the computer. The sample positions are aligned with the collimated beams very carefully before the experiment. The enriched samples of copper isotopes obtained from the ERDA research pool were in the form of metallic solid cylinders about 1.1 cm long and 2.00 cm in diameter. The samples were weighed accurately and from this the thickness of the sample was determined for $^{63,65}$Cu to be $1/n$ (b/atom) = 12.66 and 13.45, respectively, with an uncertainty of 0.1% due to the uncertainties in the measurement of its diameter and mass. The mass and chemical analyses of the samples are given in Table I.

A total cross section (or transmission) measurement requires a fast, efficient, neutron detector with low background. For the present measurements made at the 80-m flight path station, a proton-recoil plastic scintillator (NE-110)[2] was used for neutron energies above ~10 keV and a $^6$Li-glass scintillator for lower energies. The NE-110 plastic scintillator when suitably mounted on a selected RCA 4522, 12.7-cm phototube with a special base is found to be capable of detecting neutrons whose energies are only a few keV. This

TABLE I. Spectrographic analysis of the samples of copper isotopes used for the measurements. The copper isotopic content is in atomic percent. The sample contains additional contaminants in the percentage indicated.

| Isotope | Isotopic analysis Atomic (%) | Precision | Spectrographic analysis Element (%) |
|---|---|---|---|
| $^{63}$Cu | 99.86 | ±0.02 | Ca <0.07 |
| $^{65}$Cu | 0.10 | ±0.02 | Si <0.03 |
| | | | Mg <0.01 |
| | | | Other metallic elements below limit of detection. |
| | | | Assay performed before conversion and fabrication. |
| $^{63}$Cu | 0.30 | ±0.02 | Ag <0.01 |
| $^{65}$Cu | 99.70 | ±0.02 | Al <0.10 |
| | | | Ba <0.03 |
| | | | Ca <0.50 |
| | | | Fe <0.02 |
| | | | Mg <0.02 |
| | | | Na <0.02 |
| | | | Ni <0.03 |
| | | | Si <0.10 |
| | | | Sr <0.02 |
| | | | V <0.03 |
| | | | Yb <0.005 |
| | | | Other metallic elements below limit of detection. Assay performed before conversion and fabrication. |

NE-110 scintillator is superior in efficiency to the $^6$Li-glass detector above ~10 keV neutron energy, and by as much as an order of magnitude above ~50 keV. The NE-110 scintillator is very fast (3.3-nsec decay constant), and the tail produced by the $\gamma$ rays arising from the capture of neutrons by hydrogen in the target moderator is small (<0.1% for 10 keV-energy neutrons but is more important for higher energy neutrons, but $\lesssim 1\%$). The NE-110 detector is sensitive to both high energy neutrons and $\gamma$ rays. At the end of the flight path in the detector station, the detector is suspended in air in the line of sight of the 7.6-cm diameter collimated neutron beam about 1 m away from the end of the beam pipe and at a height 1.22 m above the floor. This position of the detector is chosen as a result of optimizing the "good neutron" detection against the back-scattered neutron background in the detector room.

To optimize the signal to background ratio four different pulse height "windows" are used. The data acquisition logic is set up to record the data from different windows separately with mutually exclusive characteristics. This enables only the "best data" with a high signal to background ratio from different windows to be added together at the end of the run to maintain nearly uniform statistics throughout the experimental energy range. The first window is set for neutrons with energies <200 keV, the second for 170–600 keV, the third for 400 keV–2 MeV, and the fourth window for energies >2 MeV. This arrangement isolated the contribution from the 478-keV $\gamma$ rays (produced from the neutron reaction with $^{10}$B in the pyrex of the phototube) mostly to the third window and from the 2.23-MeV $\gamma$ rays produced by neutron capture in the hydrogen of the water moderator mostly to the fourth window with less than 20% in the other three windows. This elaborate arrangement of biases was used for the accurate determination of background contributions through separate accumulation of the data from different windows.

### III. DATA PROCESSING

The transmission of neutrons as a function of energy is computed by the simple relation $T = (N_s - \mathrm{BG}_s)/(N_o - \mathrm{BG}_o)$, where $N_s$ and $N_o$ are the neutron counting rate with the sample in position and the open beam, respectively, and the BG's are the corresponding backgrounds. The true experimental counts are determined after the dead-time correction and background subtractions have been made. The background consists of two essential parts: (a) time independent and (b) time dependent. The time-independent background is determined from the counts at long flight which basically record the constant contributions due to cosmic radiations and other radiations in the laboratory. The time-dependent background is a complex function of various components. The most important of these are due to the contribution of 2.23-MeV $\gamma$ rays from neutron capture by hydrogen in the target and 478-keV $\gamma$ rays from $^{10}\mathrm{B}(n, \alpha\gamma)$ in the phototube of the detector. The mean capture time of the 478-keV $\gamma$ rays from the $^{10}\mathrm{B}(n, \alpha\gamma)$ reaction is from 1 to 2 $\mu$sec. As discussed earlier, care must be taken to isolate the contributions of the two $\gamma$ rays to the different windows. For the determination of the contribution of 478-keV $\gamma$ rays from $^{10}\mathrm{B}(n, \alpha\gamma)$, a $\mathrm{Be}^7$ source is placed near the detector (with the neutron beam shut off) and the relative contributions in different window settings are determined. Similarly, the contribution of 2.23-MeV $\gamma$ rays can be determined by placing a thick piece of polyethylene in the neutron beam, thus stopping all the neutrons reaching the detector. This background due to 2.23-MeV $\gamma$ rays is found to decay exponentially with a half-life ~18.4 $\mu$sec. From this information one can determine the background contribution for the lowest windows from the fourth window for sample in and out conditions. For these measurements the time-independent background was found to be less than 1% above 25 keV neutron energy and the time-dependent background less than 1% over the entire energy interval investigated. The transmission and cross section values as a function of neutron time-of-flight channel are calculated from the normalized background-corrected counts.

### IV. ANALYSIS OF TRANSMISSION AND CROSS SECTION DATA

The analysis of these data to extract the resonance parameters was carried out by two methods: "an area analysis of transmission data" and "a shape analysis of total cross section data." The area analysis program[3] (written for analyses of low energy resonances $\lesssim 10$ keV) uses the sum of single channel, Breit-Wigner resonances where $\sin(kR)$ has been approximated by $kR$ and includes Doppler and resolution broadening. This program is appropriate for cases where the experimental energy resolution and the Doppler widths are greater than the natural widths of the resonances. The area code searches on only $\Gamma n$ (for a fixed value of total width $\Gamma$) to determine a value of $\Gamma n$ so that the area under a transmission dip of the experimental data is equal to that calculated from the Breit-Wigner formula. A typical result of the area analysis for the resonance at ~50 keV shown in Fig. 1 is computed using the value of $\Gamma n$ determined from the code and for the assumed value of

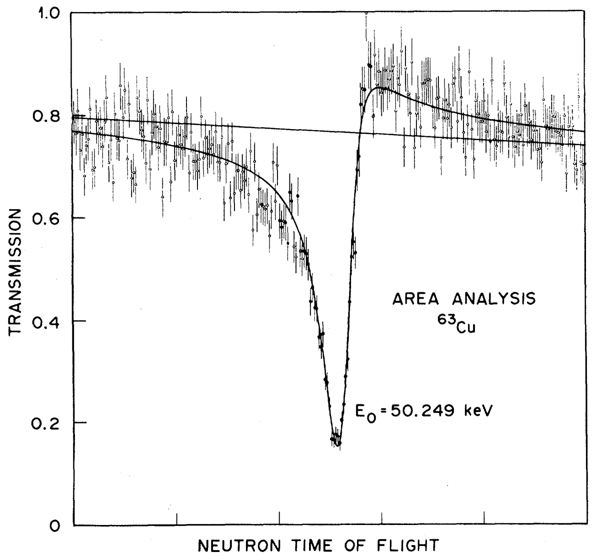


FIG. 1. An example of the area program fit to the transmission data of an isolated resonance in $^{63}$Cu at $E_0 = 50.249$ keV.

Γ. The shape analysis program is based on the single channel, multilevel $R$-matrix formalism.[4] The analysis using the area code was performed on PDP-10 and IBM360/91 computer systems of ORELA/ORNL and that of the $R$-matrix code on the UNIVAC1108/1110 computer system at the State University of New York at Albany (SUNYA). Numerous weak $s$-wave and a majority of the $p$-wave resonances were analyzed using the area code.

We have also analyzed some broad and interfering $l = 0$ resonances up to ~100 keV by the area code in order to obtain approximate values of parameters to be used as initial input for the $R$-matrix analysis. Most of the broad $s$-wave resonances must be analyzed by the multilevel $R$-matrix code. The results of the $R$-matrix analysis are shown in Figs. 2, 3, and 4. For the $R$-matrix analysis an averaging of data over a number of channels has been done in order to smooth out the cross section between broad resonances, since the weak $s$-wave and $p$-wave resonances were not included in this analysis. As an illustration of the

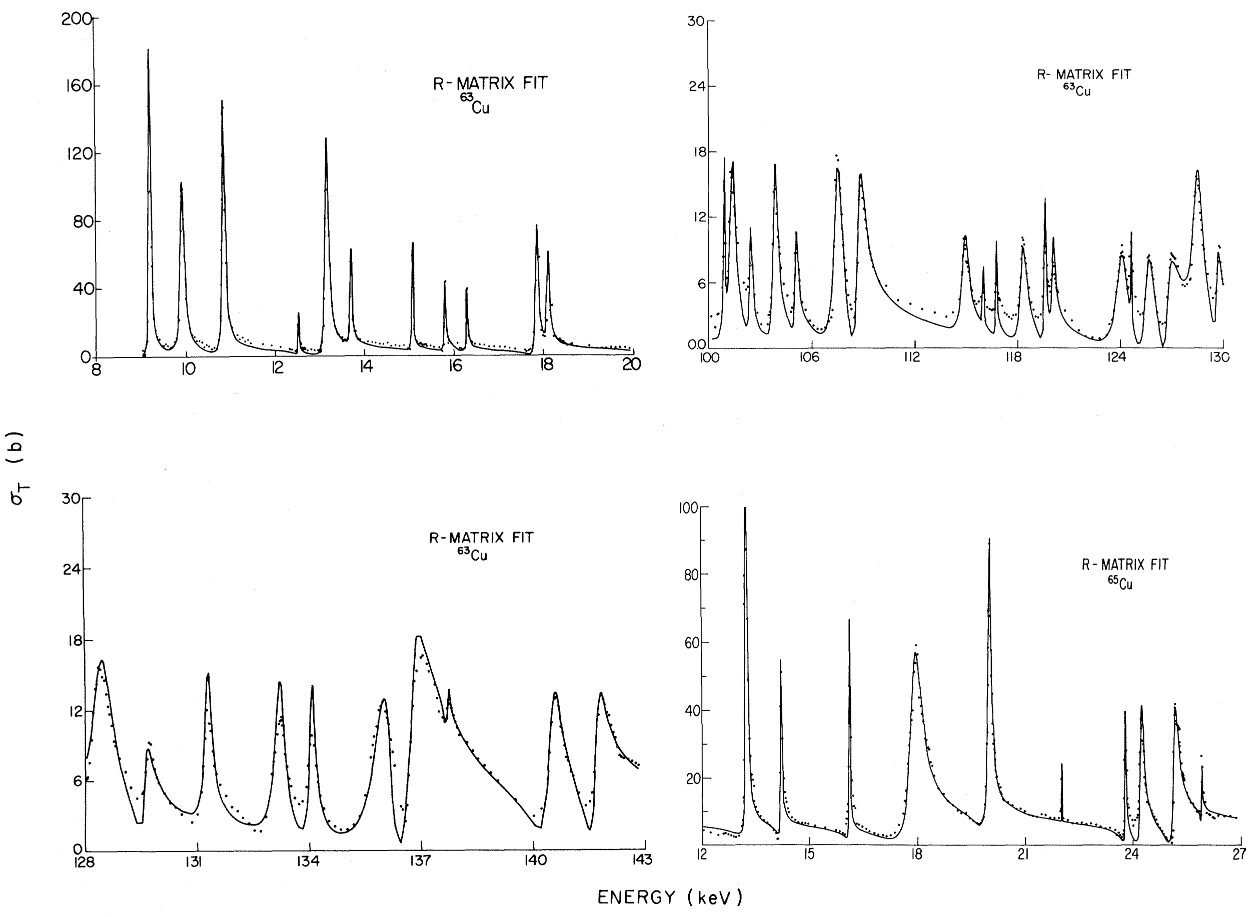


FIG. 2. $R$-matrix multilevel fit to the data of $^{63}$Cu and $^{65}$Cu in the lowest and highest energy regions investigated.

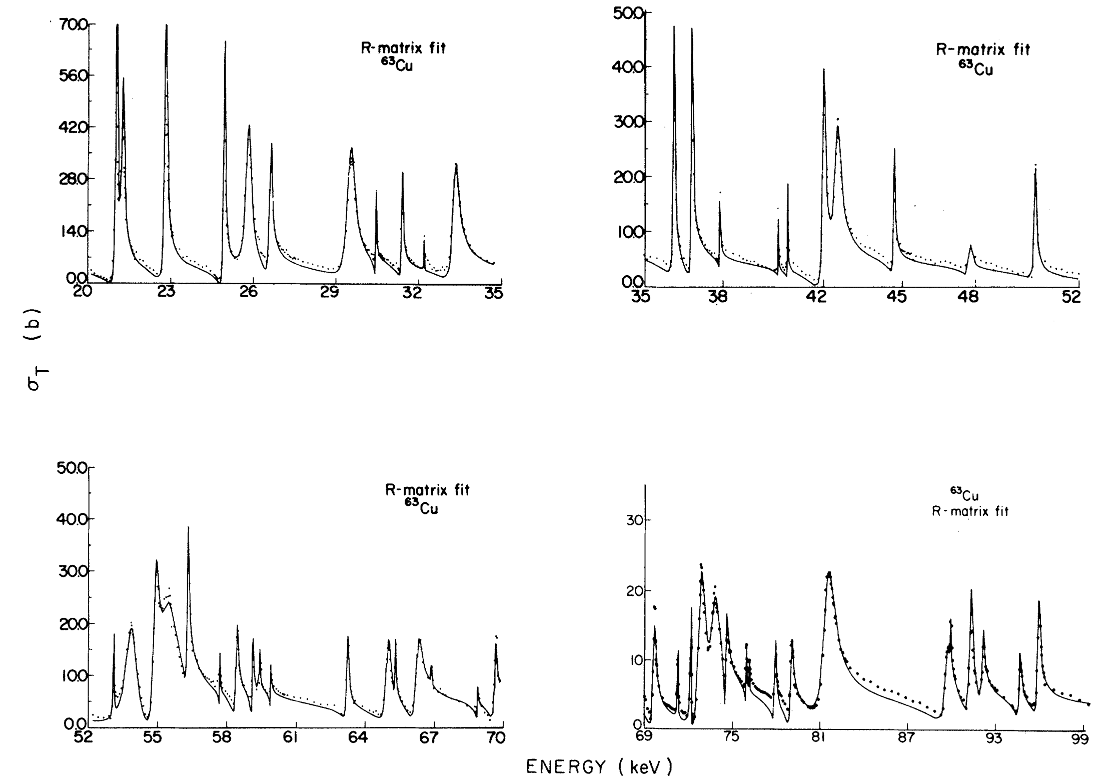


FIG. 3. $R$-matrix multi-level fit to the total cross section data in $^{63}$Cu.

energy resolution and quality of the present data in the energy interval of 140–154 keV, the unaveraged cross section data for $^{63}$Cu are shown in Fig. 5.

A visual observation of the comparison of the experimental data with the fit of the $R$-matrix multilevel analysis shows that in some energy regions, the fit is rather poor in between resonances, although it is quite good on the peaks and shoulders of the resonances. The poor fit between resonance regions can partially be explained as resulting from the fact that the data have been averaged over many channels which included weak $s$-wave and $p$-wave resonances and the contribution of these weak resonances was not included in the $R$-matrix analysis.

The $R$-matrix analysis includes contributions to cross sections between resonances, not only from the wings of the resonances but also from the effect of the particular choice of the coefficients $A_J$, $B_J$, $\bar{a}$, and $E_{1/2}$ used in the expansion of the $R$ function.[4] The parameter $\bar{a}$ is the nuclear radius chosen and $E_{1/2}$ is the midpoint of the energy region being analyzed.

In the analysis procedure, we analyze the total cross section data first up to a few tens of keV with the inclusion of thermal cross section values of $\sigma_{\rm coh}$, $\sigma_s$, and $\sigma_{n\gamma}$. This analysis provides us the values of $A_J$, $B_J$, and the parameters $(E_0, \Gamma_n)$ of any bound resonances needed to fit these data. $A_J$ and $B_J$ are given as

$$A_J = R^\infty + \sum_\mu \frac{\gamma_{\mu J}}{E_{\mu J} - E_{1/2}}, \quad B_J = \sum_\mu \frac{\gamma_{\mu J}{}^2}{(E_{\mu J} - E_{1/2})^2}.$$

Hence $A_J$ includes not only the contribution from the energy regions far outside the range of analysis ($R^\infty$), but also the contributions from the known resonances in the vicinity of the energy range analyzed $[\sum_\mu \gamma_{\mu J}{}^2/(E_{\mu J} - E_{1/2})]$. Therefore, if the analysis is extended to higher energy regions it is necessary to reduce the value of $A_J$ and $B_J$ by an appropriate amount.

In our experience with this type of analysis we have observed that the fit in the region between resonances is also sensitive to the value of $E_{1/2}$ chosen for the analysis. As the data are extended to the higher energy regions, the appropriate value of $E_{1/2}$ is found to be lower than the midenergy for a good fit. Besides, if an energy region between $E_1$ and $E_2$ is analyzed where $E_1 \gg 0$, the value of $E_{1/2}$ is not clearly defined. One usually obtains a better fit in the region between resonances when $E_1 \simeq 0$. Hence, it is not obvious that a good fit obtained between two isolated energy regions with different values of $A_J$, $B_J$, and $E_{1/2}$ would be

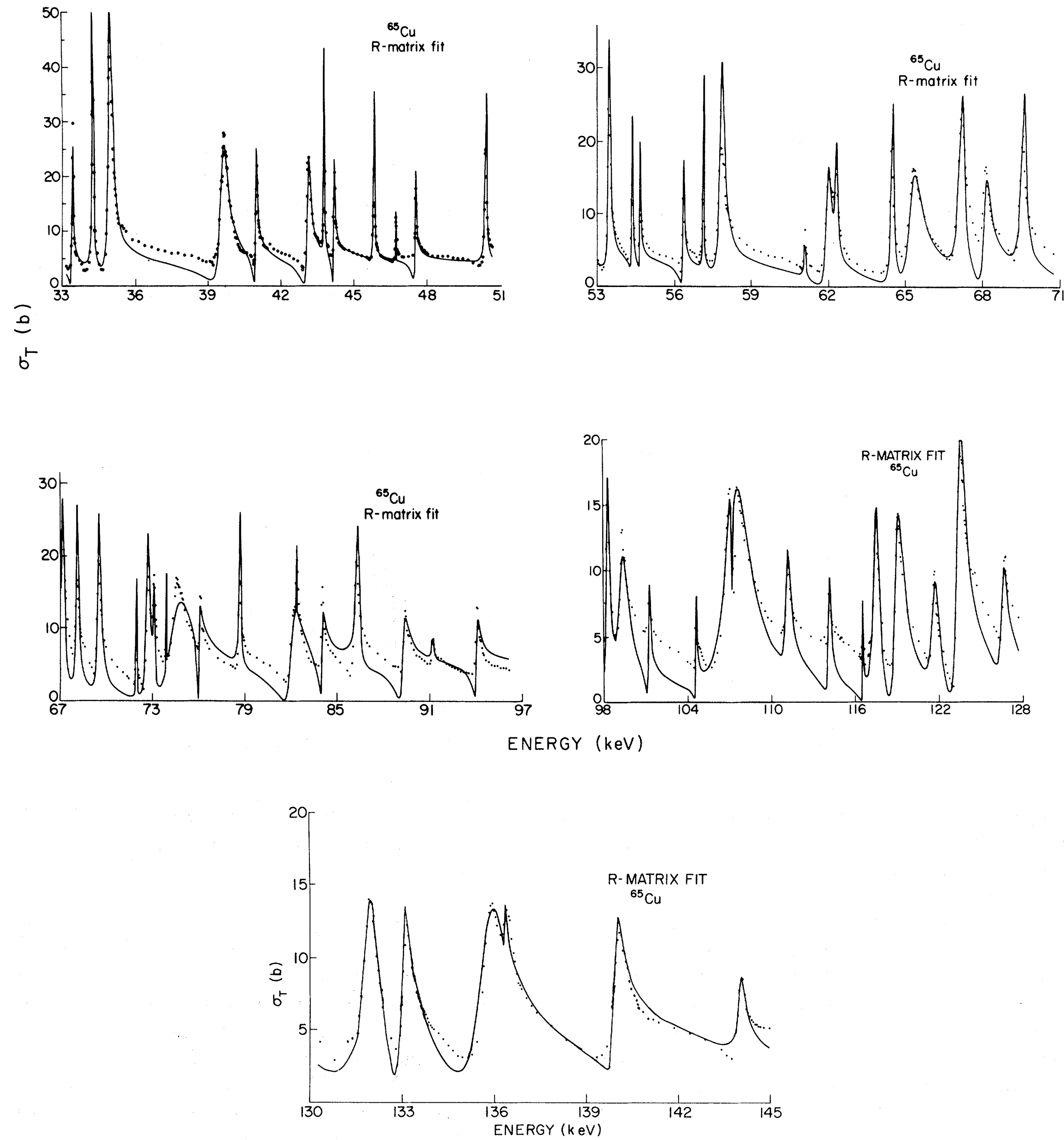


FIG. 4. $R$-matrix multi-level fit to the total cross section data in $^{65}$Cu.

physically meaningful unless one assumes some dependence of strength function and effective nuclear radius on the neutron energy.

The neutron widths obtained for most of the $s$-wave resonances from this analysis are in general insensitive to the fits in between resonances; however, occasional poor fits between resonances can affect these values significantly. These considerations should be taken into account in the estimation of uncertainties in the values of $\Gamma_n$.

The initial inputs for the resonance parameters for $R$-matrix analysis were taken from the previously analyzed transmission data by area analysis or from published results.[5-9] The values of the known thermal cross sections[10] along with the present experimental cross sections up to about 10 keV were first analyzed with an emphasis on fitting the thermal cross section data. This helped determine the $A_J$ and $B_J$ coefficients of the $R$ function. Having determined these coefficients, more higher energy data were included with appropriate changes in the values of $A_J$ and $B_J$.

The total cross sections at low energies, down to ~50 eV, of the two copper isotopes were mea-

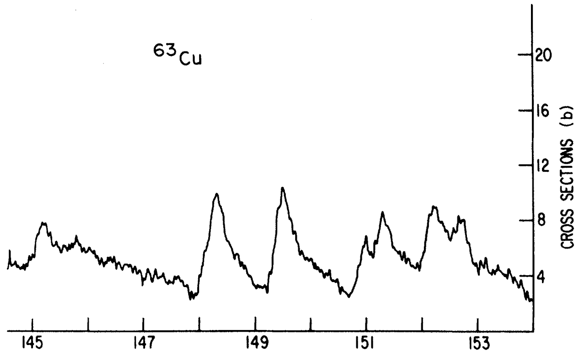


FIG. 5. The unaveraged total cross section data for $^{63}Cu$ between 140-154 keV as an illustration of the quality of the data.

sured using the $^6Li$ glass scintillator. The measured $\sigma_T$ for $^{63}Cu$ and $^{65}Cu$ isotopes at 50 eV are $(5.4 \pm 0.2)$ b and $(13.0 \pm 0.2)$ b, respectively. No attempt was made to analyze the resonances below 10 keV since the resonance parameters at such low energies have been previously determined quite accurately by other authors.[7,9] When, however, the parameters of the observed low energy resonances of $^{65}Cu$ are used in the $R$-matrix analysis to calculate the cross section at 50 eV and at thermal energies, one obtains a value $\sigma_T = 8.5$ b at 50 eV. This is much smaller than that observed. Moreover, for a chosen value of $\Gamma_\gamma = 0.4$ eV for the resonances one obtains a value of $\sigma_{n\gamma} = 0.003$ b at thermal energy as compared to the observed value of $\sigma_{n\gamma} = 2.17$ b. Hence it is obvious that there is a bound resonance (or resonances) giving rise to large scattering and capture cross section at low energies. We have used the $R$-matrix code to determine the parameters of such bound resonance and we obtain the parameters as $E_0 = -180$ eV, $\Gamma_n = 0.87$ eV. Although these parameters provide a value for $\sigma_{n\gamma} = 2.16$ b in excellent agreement with the observed value, the agreement with the coherent scattering cross section and $\sigma_s$ can only be obtained if the effective nuclear radius for $^{65}Cu$ is much larger than 6 fm. A good agreement with the observed data up to 10 keV is obtained if the coefficients of $A_J$ and $B_J$ for the two spin states are used as given in Table II.

The spins of both copper nuclei are $\frac{3}{2}^-$. Hence the interaction of $s$-wave neutrons populates states in the compound nucleus with spins $1^-$ and $2^-$. The assignment of the spin to a particular resonance is made with the following points considered simultaneously. The peak cross section at resonance is given as $\sigma_{peak} = 4\pi\lambda\!\!\!^{-2}(ag/\Gamma)\Gamma_n[(A+1)/A]^2$ (where $g = \frac{3}{8}$ or $\frac{5}{8}$ for $J = 1$ or 2 and $a$ is the isotopic abundance). Hence, if the peak $\sigma_T$ values of resonances with $\Gamma_n \gg \Gamma_\gamma$ are measured accurately, one can easily determine their $g$ values or $J$ values. The second important effect observed is the interference minima between resonances of the same spin. The cross sections from resonances of different spins add incoherently. Hence, from these two considerations it was possible to make the proper assignment of $J$ values to most of the $s$-wave resonances. For the data below about 40 keV obtained from the isotopic samples of copper, the true peak cross section was not observed because the samples were too thick ($1/n = 12.66$ b/atom and $1/n = 13.45$ b/atom for $^{63}Cu$ and $^{65}Cu$, respectively). To determine the true peak cross sections at resonances, a sample of natural copper with a smaller thickness ($1/n_{Cu} = 74.2$ b/atom) was used for measurement. The peak cross section values with appropriate isotopic abundance were adapted for the isotopic data on the peaks of the resonances.

TABLE II. Values of the coefficients $A_J$ and $B_J$ as obtained from the $R$-matrix analysis of $^{63}Cu$ and $^{65}Cu$ data.

| | $l=0$, $J=1$ | $l=0$, $J=2$ | $l=1$ | | $E_{min}$ keV | $E_{max}$ keV |
|---|---|---|---|---|---|---|
| | | | $^{63}Cu$ | | | |
| $A_J$ | $-0.1\times10^{-2}$ | $0.85\times10^{-1}$ | 0.10 | 0.10 | 0 | 20 |
| $B_J$ | $0.5\times10^{-5}$ | $0.5\times10^{-5}$ | $0.5\times10^{-8}$ | $0.5\times10^{-8}$ | | |
| $A_J$ | $-0.2\times10^{-2}$ | $0.94\times10^{-1}$ | 0.10 | 0.10 | 32 | 70 |
| $B_J$ | $0.5\times10^{-5}$ | $0.5\times10^{-5}$ | $0.5\times10^{-8}$ | $0.5\times10^{-8}$ | | |
| | | | $^{65}Cu$ | | | |
| $A_J$ | $-0.79$ | $0.10\times10^{-1}$ | 0.10 | 0.10 | 0 | 27 |
| $B_J$ | $0.5\times10^{-5}$ | $0.4\times10^{-4}$ | $0.5\times10^{-8}$ | $0.5\times10^{-8}$ | | |
| $A_J$ | $-0.63$ | $0.10\times10^{-1}$ | 0.10 | 0.10 | 25 | 52 |
| $B_J$ | $0.5\times10^{-5}$ | $0.4\times10^{-4}$ | $0.5\times10^{-8}$ | $0.5\times10^{-8}$ | | |

Spin assignments of $p$-wave resonances could not be made with confidence using the area code since in general $\Gamma_n$ is small compared to the energy resolution and Doppler width. Hence only the values of $g\Gamma_n$ are given in Tables V and VIII. In addition to the $p$-wave resonances given in Tables V and VIII, the following additional $p$-wave resonances have been observed in the present measurements. These resonances are too weak in transmission to be analyzed accurately; however, they have been analyzed in the accompanying paper on capture measurements.[14] For $^{63}$Cu the small resonances observed in transmission are at energies $E_0$ = 14 127, 14 555, 16 054, 32 836, 35 744, 38 387, 40 397, 43 882, 45 131, 45 544, 45 803, 46 561, 48 203, 52 849, 56 930, 57 133, 60 639, 62 168, 67 289, 68 074, 69 816, 76 380, 77 528, 77 711, 79 441, 83 010, 98 295, and 98 798 eV. For $^{65}$Cu the small resonances observed in transmission are at energies (eV) 12 133, 13 673, 16 730, 25 392, 29 210, 30 900, 32 205, 34 660, 40 762, 44 760, 47 230, 59 597, 61 450, 63 573, 80 545, 84 381, 84 624, 89 682, 94 876, and 99 000. The $R$-matrix analysis of the cross section data provides estimates of $E_\lambda$, $\Gamma_{\lambda J n}$, and $J$ values for the $s$-wave resonances. $R$-matrix fits to the total cross sections for $^{63}$Cu in the energy range (20.0–99.0) keV are shown in Fig. 3 and for $^{65}$Cu in the energy range (33.0–128.0) keV are shown in Fig. 4. Numerical least square analysis has been employed to determine the parameters which give the best fit to the cross section. The best estimates are obtained on the basis of the usual method of minimizing the $\chi^2$. The error matrix resulting from the least square analysis supplies as its elements the variances and the covariances associated with the best estimates of the variables.

## V. DISCUSSION OF RESULTS

### $^{63}$Cu(n,n)

The resonance parameters obtained from these analyses of the data from 10 to 150 keV are given in Tables III–V. These results are $E_0$, $\Gamma_n$, and $J^\pi$ values as obtained from the area and shape analyses. The $E_0$'s are $R$-matrix eigenvalues for $s$-wave resonances which are lower than the energies at the peak cross sections. The uncertainty in the energy values quoted is determined from the observation of fits to the data by varying the energy. It is difficult to determine the uncertainty in the $\Gamma_n$ values. In general, our $R$-matrix program does not provide an estimate of these uncertainties. The uncertainty is estimated by comparing the fitted and measured cross sections by small variations of $\Gamma_n$. We estimate that the uncertainties in the values of $\Gamma_n$ are in general less than 10% for most

TABLE III. Resonance parameters of $s$-wave levels obtained from the $R$-matrix analysis of $^{63}$Cu ($J = 1$).

| $E_0$ (eV) | $\Delta(E_0)$ ± (eV) | $\Gamma_n$ (eV) | $\Delta\Gamma_n$ ± (eV) |
|---|---|---|---|
| 12 520 | 50 | 12 | 1 |
| 13 695 | 60 | 32 | 4 |
| 15 080 | 70 | 24 | 3 |
| 15 805 | 80 | 24 | 4 |
| 16 293 | 50 | 19 | 3 |
| 18 110 | 50 | 54 | 6 |
| 21 225 | 75 | 120 | 11 |
| 25 800 | 80 | 307 | 32 |
| 26 590 | 50 | 115 | 14 |
| 29 500 | 50 | 327 | 31 |
| 30 450 | 50 | 21 | 3 |
| 31 390 | 70 | 58 | 6 |
| 33 303 | 80 | 282 | 25 |
| 37 930 | 40 | 20 | 4 |
| 40 218 | 50 | 11 | 2 |
| 40 585 | 70 | 17 | 2 |
| 42 500 | 60 | 270 | 30 |
| 44 750 | 55 | 67 | 9 |
| 47 650 | 55 | 46 | 5 |
| 50 250 | 50 | 111 | 13 |
| 53 764 | 60 | 605 | 51 |
| 55 380 | 80 | 780 | 58 |
| 57 700 | 90 | 19 | 3 |
| 58 410 | 90 | 117 | 11 |
| 59 110 | 90 | 49 | 6 |
| 59 900 | 50 | 16 | 1.5 |
| 63 220 | 50 | 101 | 10 |
| 64 970 | 70 | 262 | 16 |
| 66 280 | 80 | 304 | 27 |
| 68 860 | 60 | 24 | 3 |
| 69 636 | 40 | 214 | 19 |
| 73 728 | 30 | 647 | 60 |
| 74 580 | 80 | 99 | 10 |
| 77 953 | 60 | 77 | 8 |
| 79 034 | 45 | 172 | 15 |
| 89 677 | 75 | 430 | 160 |
| 92 120 | 20 | 169 | 16 |
| 94 649 | 40 | 133 | 12 |
| 102 420 | 40 | 147 | 15 |
| 105 050 | 50 | 191 | 21 |
| 114 850 | 50 | 426 | 40 |
| 116 760 | 60 | 76 | 9 |
| 118 250 | 50 | 400 | 40 |
| 120 050 | 100 | 168 | 16 |
| 123 920 | 100 | 790 | 80 |
| 125 550 | 95 | 480 | 52 |
| 126 850 | 85 | 563 | 55 |
| 129 620 | 50 | 211 | 21 |
| 136 820 | 100 | 406 | 50 |
| 137 700 | 90 | 31 | 4 |
| 145 110 | 110 | 27 | 6 |

of the well fitted $s$-wave resonances but is about 20 to 30% for most of the $p$-wave and weak $s$-wave resonances analyzed by this program. For the weak resonances analyzed by the area code, the uncertainties in $g\Gamma_n$ are somewhat smaller and are determined by the program.

Measurements of the total cross section in these nuclei have been made by other research groups in the last few years. The most notable among these are the Columbia measurements[9] made at the Nevis Synchrocyclotron Laboratories, the measurements of Alves *et al.*[7] made with a linear accelerator, and that of Beer, Spencer, and Rohr[8] made with a Van de Graaff generator using the time-of-flight technique and a nominal resolution of 0.04 nsec/m. The cross section data of the first two experimenters have been analyzed from a few hundred eV up to 50 and 30 keV, respectively, whereas the measurements of Beer *et al.*[8] were performed in the energy interval of 35 to 150 keV. Our present results cover the entire energy region up to 150 keV. Hence, these comparisons are made in two separate energy regions, i.e., up to 35 keV and from 35 to 150 keV. A comparison of the results below 35 keV shows that our energies are consistently higher than the results of Alves *et al.*[7] but are in good agreement with the Columbia re-

TABLE IV. Resonance parameters of $s$-wave levels obtained from the $R$-matrix analysis of $^{63}$Cu ($J=2$).

| $E_0$ (eV) | $\Delta(E_0)$ ± (eV) | $\Gamma_n$ (eV) | $\Delta\Gamma_n$ ± (eV) |
|---|---|---|---|
| 10 839 | 50 | 56 | 6 |
| 13 150 | 50 | 74 | 8 |
| 17 855 | 60 | 50 | 6 |
| 21 005 | 75 | 75 | 7 |
| 22 790 | 60 | 100 | 11 |
| 24 905 | 50 | 60 | 7 |
| 36 135 | 70 | 75 | 8 |
| 36 833 | 75 | 75 | 10 |
| 41 980 | 50 | 130 | 12 |
| 54 900 | 50 | 220 | 20 |
| 56 300 | 80 | 98 | 11 |
| 59 420 | 65 | 16 | 3 |
| 65 300 | 75 | 20 | 3 |
| 72 170 | 70 | 72 | 8 |
| 72 790 | 70 | 415 | 45 |
| 75 940 | 50 | 17 | 5 |
| 81 440 | 50 | 825 | 90 |
| 89 940 | 50 | 10 | 6 |
| 91 276 | 60 | 228 | 25 |
| 95 885 | 60 | 188 | 20 |
| 101 320 | 80 | 386 | 40 |
| 103 800 | 70 | 290 | 50 |
| 107 400 | 75 | 500 | 75 |
| 108 720 | 75 | 460 | 70 |
| 119 580 | 75 | 130 | 25 |
| 128 320 | 70 | 660 | 70 |
| 131 230 | 50 | 230 | 30 |
| 133 130 | 60 | 284 | 40 |
| 134 030 | 50 | 150 | 30 |
| 135 850 | 60 | 735 | 100 |
| 136 800 | 70 | 731 | 200 |
| 140 480 | 50 | 320 | 50 |
| 141 700 | 80 | 277 | 50 |
| 148 350 | 100 | 280 | 50 |
| 149 500 | 100 | 260 | 40 |

TABLE V. Resonance parameters of $p$-wave levels obtained from the area analysis of $^{63}$Cu data. The energies of additional $p$-wave resonances too weak to be analyzed are given elsewhere.

| $E_0$ (eV) | $g\Gamma_n$ (eV) | $\Delta g\Gamma_n$ (eV) |
|---|---|---|
| 12 525 | 3.8 | 0.8 |
| 21 730 | 1.2 | 0.5 |
| 23 327 | 1.2 | 0.5 |
| 23 612 | 1.3 | 0.5 |
| 32 201 | 3.8 | 0.8 |
| 34 063 | 3.4 | 0.7 |
| 34 268 | 2.1 | 0.6 |
| 34 449 | 2.1 | 0.5 |
| 39 388 | 3.5 | 0.5 |
| 47 378 | 5.1 | 1.0 |
| 53 111 | 15.7 | 1.1 |
| 60 432 | 4.1 | 0.7 |
| 62 635 | 2.5 | 0.6 |
| 66 876 | 5.3 | 0.6 |
| 70 537 | 6.1 | 0.9 |
| 71 278 | 23 | 1 |
| 76 155 | 9 | 1.4 |
| 84 455 | 11.2 | 1 |
| 85 860 | 6.6 | 1 |
| 87 294 | 7.8 | 1.9 |
| 87 500 | 6.4 | 0.9 |
| 88 810 | 3.8 | 0.8 |
| 93 188 | 8.4 | 1 |
| 93 625 | 13.1 | 1.2 |
| 95 213 | 13.8 | 1.4 |
| 95 483 | 11.4 | 1.3 |
| 96 578 | 4.2 | 1.0 |
| 96 897 | 15.5 | 1.4 |
| 100 940 | 57 | 2 |
| 102 020 | 20 | 2 |
| 103 230 | 8.2 | 1 |
| 110 180 | 11.0 | 1.5 |
| 111 280 | 10.2 | 1.4 |
| 112 040 | 29 | 2 |
| 116 020 | 3.9 | 0.9 |
| 121 120 | 16 | 1.6 |
| 121 630 | 8.4 | 1.2 |
| 122 370 | 9.8 | 1.1 |
| 124 560 | 39 | 4 |
| 130 440 | 6.2 | 1.2 |
| 139 840 | 18 | 2 |
| 143 220 | 18 | 2 |
| 143 670 | 21 | 2 |
| 144 110 | 6.3 | 1.8 |

sults.[9] There are some disagreements in the assignment of $J$ values to the individual resonances, but the overall agreement between $\Gamma_n$ values seems to be quite good.

Above 35 keV, the only other measurement for comparison is that of Beer *et al.* The agreement between our results and that of Beer *et al.*[8] is in general fair. The points of difference are, however, discussed in the following: Beer *et al.* assign $J=1$ spin to the resonances at 36.135, 119.58, 134.03, and 149.5 keV; we assign these to $J=2$. They assign $J=2$ to the resonances at 47.65, 57.7, 58.41, 59.11, 63.22, 92.12, 114.85, and 126.85 keV; we assign these to $J=1$. Beer *et al.* have assigned $l>0$ to resonances at energies 37.95, 59.6, 59.8, 72.2, 125.9, and 131.4 keV, whereas in the present analysis they were assigned as $s$-wave resonances at energies 37.930 keV ($J=1$), 59.420 keV ($J=2$), 59.900 keV ($J=1$), 72.170 keV ($J=2$), 125.55 keV ($J=1$), and 131.23 keV ($J=2$). Furthermore, their assignment of $s$ wave to the resonances at 39.388, 53.111, 71.278, 95.483, and 100.94 keV is not matched by us as we have assigned those resonances as $p$ wave. Also, there is a doublet resolved by us at 95.5 keV (95.213 and 95.483 keV), both $p$ wave. They report singlets at the energies 65.0, 89.7, and 119.5 keV. We have observed and analyzed doublets at these energies with energy values of 64.97 keV ($J=1$) and 65.3 keV ($J=2$), 89.677 keV ($J=1$) and 89.94 keV ($J=2$), 119.58 keV ($J=2$) and 120.05 keV ($J=1$). There are certain resonances clearly resolved by us which are not reported by Beer *et al.* These are at energies 102.42 keV ($J=1$), 116.76 keV ($J=1$), 129.62 keV ($J=1$), 145.11 keV ($J=1$) and 148.35 keV ($J=2$). Beer *et al.*, however, report resonances at energies 73.3, 100.2, 146.2, and 147.9 keV which are not confirmed by us. We see only a small fluctuation in $\sigma_T$ which we consider to be statistical in nature. Also, they report a pair of resonances at 142.1 keV ($l=1$) and at 142.7 keV ($l=1$, $J=2$), whereas we observe only one at 141.7 keV ($l=0$, $J=2$).

### $^{65}$Cu(*n,n*)

Above an energy of about 34 keV the resonance parameters are compared with the results of Beer *et al.*[8] Agreement between the present results and those of Beer *et al.*[8] is only fair for resonance energies and neutron widths, and the assignments of some of the spins disagree. (See Tables VI–VIII.) Resonances reported by them at energies 105.5 keV ($\Gamma_n=85$) and 130 keV ($\Gamma_n=110$) are seen in the present measurement only as statistical fluctuation in the $\sigma_T$ values. Their assignment of $J=1$ to the following resonances at energies 45.830, 50.460, 57.130, 69.522, 78.680, 98.275, 107.300, and 117.440 keV is in disagreement with the present analysis where all these have been assigned as $J=2$. Similarly, their assignment of $J=2$ to the following resonances at energies 40.970, 84.076, 89.360, 94.070, 99.245, 104.600, 121.630, and 126.550 keV is different from the present result of $J=1$. They assign resonances at 43.765 keV ($J=2$), 54.680 keV ($J=2$), 111.120 keV ($J=1$), and 114.140 keV ($J=1$) to $l>0$, whereas in the present analysis they are attributed to $s$-wave neutron interaction. Furthermore, their assignment of $l=0$ to the 46.735-keV resonance is disputed by us, since we assign it to $l=1$ in the present analysis.

TABLE VI. Resonance parameters of $s$-wave levels as obtained from the $R$-matrix analysis of $^{65}$Cu ($J=1$).

| $E_0$ (eV) | $\Delta(E_0)$ ± (eV) | $\Gamma_n$ (eV) | $\Delta\Gamma_n$ ± (eV) |
|---|---|---|---|
| 14 200 | 20 | 28 | 4 |
| 16 100 | 50 | 40 | 5 |
| 17 910 | 30 | 435 | 40 |
| 23 802 | 30 | 31 | 4 |
| 24 250 | 40 | 111 | 15 |
| 25 185 | 25 | 167 | 20 |
| 25 918 | 30 | 8 | 3 |
| 33 414 | 40 | 48 | 5 |
| 39 590 | 50 | 300 | 40 |
| 40 970 | 60 | 60 | 10 |
| 43 119 | 60 | 150 | 20 |
| 44 184 | 50 | 45 | 15 |
| 47 540 | 50 | 44 | 10 |
| 56 351 | 40 | 56 | 8 |
| 57 779 | 70 | 300 | 60 |
| 61 980 | 70 | 225 | 30 |
| 65 280 | 70 | 530 | 70 |
| 68 099 | 80 | 240 | 50 |
| 73 115 | 80 | 130 | 20 |
| 74 540 | 40 | 1200 | 300 |
| 76 075 | 70 | 130 | 20 |
| 82 180 | 80 | 600 | 100 |
| 84 067 | 70 | 220 | 60 |
| 89 360 | 60 | 295 | 80 |
| 91 207 | 80 | 38 | 10 |
| 94 070 | 70 | 200 | 60 |
| 99 245 | 50 | 570 | 100 |
| 101 250 | 50 | 75 | 30 |
| 104 600 | 60 | 90 | 20 |
| 111 120 | 80 | 370 | 50 |
| 114 140 | 40 | 190 | 30 |
| 116 540 | 50 | 60 | 15 |
| 121 630 | 30 | 585 | 80 |
| 123 350 | 50 | 315 | 50 |
| 126 550 | 100 | 400 | 70 |
| 133 080 | 70 | 695 | 150 |
| 136 350 | 50 | 24 | 10 |
| 139 940 | 40 | 640 | 150 |
| 140 870 | 100 | 80 | 20 |
| 143 950 | 50 | 250 | 30 |

A resonance observed in the present measurement at 116.40 keV ($J=1$) is not reported by them. We observe a pair of resonances at 72.685 keV ($J=2$) and 73.145 keV ($J=1$), whereas Beer *et al.* report only one resonance at 72.8 keV.

We have confidence in the spin assignment of most of the $s$-wave levels in the present work made from the consideration of observed peak cross sections in conjunction with the resonance to resonance interference effect. Some resonances ascribed to $p$ wave by Beer *et al.*,[8] have been assigned as $s$ wave in the present work based on the fact that when a relatively weaker $s$-wave resonance is situated in between two strong $s$-wave resonances it has been observed[11] to lose asymmetry almost completely (characteristic shape of $s$-wave resonances) and, therefore, may cause an ambiguous assignment as a $p$-wave resonance.

Hence, it appears that there are many resonances whose spin and parity assignments are in disagreement with earlier measurements. Since correct assignments of spins and parities are important for the investigation of average properties such as level spacings, width distributions, and strength functions, the present measurements in view of the superior resolution (a factor of about 8) provide these values more accurately than the earlier measurements.

TABLE VII. Resonance parameters of $s$-wave levels as obtained from the $R$-matrix analysis of $^{65}$Cu ($J=2$).

| $E_0$ (eV) | $\Delta(E_0)$ $\pm$(eV) | $\Gamma_n$ (eV) | $\Delta\Gamma_n$ $\pm$(eV) |
|---|---|---|---|
| 13 240 | 20 | 58 | 6 |
| 20 040 | 40 | 93 | 15 |
| 34 240 | 40 | 71 | 8 |
| 34 940 | 40 | 185 | 15 |
| 43 765 | 60 | 36 | 6 |
| 45 830 | 30 | 42 | 5 |
| 50 412 | 15 | 70 | 10 |
| 53 460 | 60 | 95 | 10 |
| 54 362 | 60 | 25 | 5 |
| 54 680 | 70 | 22 | 5 |
| 57 130 | 30 | 30 | 8 |
| 64 485 | 70 | 125 | 15 |
| 67 140 | 40 | 275 | 25 |
| 69 522 | 25 | 225 | 25 |
| 72 685 | 50 | 275 | 25 |
| 78 680 | 70 | 130 | 15 |
| 86 300 | 30 | 275 | 35 |
| 98 275 | 70 | 275 | 25 |
| 106 980 | 70 | 900 | 150 |
| 107 300 | 90 | 700 | 140 |
| 117 440 | 85 | 425 | 50 |
| 118 990 | 90 | 500 | 60 |
| 123 400 | 100 | 680 | 75 |
| 131 860 | 60 | 500 | 60 |
| 135 680 | 80 | 750 | 150 |
| 149 100 | 100 | 450 | 80 |

## VI. STATISTICAL DISTRIBUTION OF RESONANCE PARAMETERS

### A. $s$-wave neutron reduced width distribution

The $s$-wave neutron width distribution was studied first separately with the data of the separated isotopes and then added together to enhance the statistics. The results are plotted for comparison in Fig. 6. The histogram represents the experimental number of widths and the smooth curves are theoretical distributions as labeled. The fit to the Porter-Thomas distribution[12] appears good as expected, except there is some discrepancy in the

TABLE VIII. Resonance parameters of $p$-wave levels as obtained from the area analysis of $^{65}$Cu data. The energies of additional $p$-wave resonances too weak to be analyzed here are given elsewhere.

| $E_0$ (eV) | $g\Gamma_n$ (eV) | $\Delta g\Gamma_n$ (eV) |
|---|---|---|
| 19 366 | 1.0 | 0.3 |
| 22 028 | 4.1 | 0.6 |
| 29 138 | 2.4 | 0.6 |
| 30 949 | 2.9 | 0.6 |
| 32 434 | 1.8 | 0.6 |
| 33 657 | 1.6 | 0.8 |
| 46 873 | 5.6 | 0.6 |
| 49 747 | 3.0 | 0.4 |
| 50 767 | 3.3 | 0.5 |
| 52 887 | 2.7 | 0.4 |
| 58 354 | 5.5 | 0.7 |
| 61 105 | 4.7 | 0.7 |
| 62 328 | 20.4 | 0.7 |
| 68 660 | 5.7 | 0.8 |
| 70 187 | 3.6 | 0.6 |
| 71 970 | 12.7 | 0.9 |
| 73 907 | 3.7 | 0.9 |
| 76 932 | 5.8 | 1.1 |
| 77 235 | 5.8 | 0.9 |
| 79 430 | 3.6 | 0.9 |
| 83 032 | 14.7 | 7.0 |
| 83 340 | 13.0 | 6.0 |
| 88 103 | 4.6 | 1.0 |
| 89 935 | 5.4 | 1.1 |
| 92 806 | 3.1 | 1.3 |
| 94 325 | 8.4 | 1.0 |
| 96 493 | 12.1 | 1.4 |
| 97 068 | 10.3 | 1.2 |
| 101 420 | 7.0 | 1.0 |
| 102 300 | 16.4 | 1.6 |
| 103 140 | 19.2 | 1.9 |
| 110 390 | 6.0 | 1.4 |
| 117 030 | 10.3 | 1.8 |
| 118 100 | 9.2 | 1.2 |
| 127 390 | 9.9 | 1.5 |
| 133 770 | 23.4 | 1.6 |

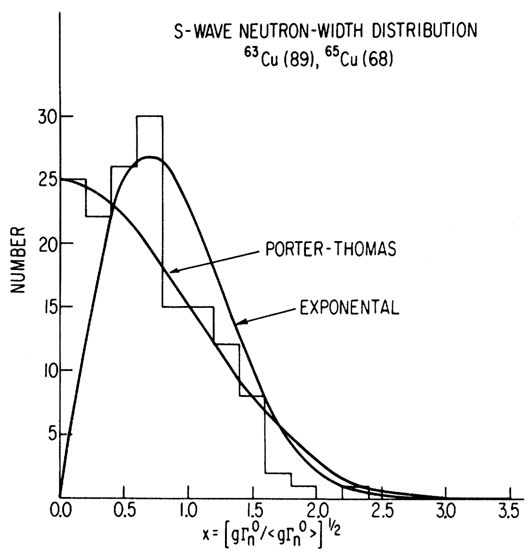


FIG. 6. The combined results of $s$-wave neutron reduced width distribution for $^{63}$Cu and $^{65}$Cu and its comparison with the theoretical distributions.

interval corresponding to 0.4 to 0.8 times $\langle g\Gamma_n^0\rangle$, which is most likely statistical in nature.

### B. $s$-wave level spacing distribution

The spacing distribution of levels at high excitation energies of complex nuclei has been investigated in great detail by many authors. Such studies in even-even nuclei are much less ambiguous and hence are more reliable for testing the relevant theories. We have attempted to make this investigation in the present nuclei more from the interest of determining if certain levels were missed or wrongly assigned as regards their spins and parities than from the interest of testing these theories.

$s$-wave level spacing distributions for separated isotopes were studied for the two spin states separately and then added together and plotted for comparison with the theoretical predictions in Figs. 7 and 8 for $^{63}$Cu and $^{65}$Cu, respectively. Experimentally observed level spacings for $^{63}$Cu seem to fit better with the Wigner distribution than with the random distribution of levels; however, there is a larger number of spacings in the interval of $x$ from 0.2 to 0.4. The level spacing distribution for $^{65}$Cu is in poor agreement with that of the Wigner distribution. There is an excess of number of levels with very small spacings ($x$ from 0.0 to 0.2 over that predicted by the Wigner distribution. Thus the present results appear to indicate that either some assignments of spins and parities may be wrong or might have been assigned as $p$ wave. One could perhaps study the level

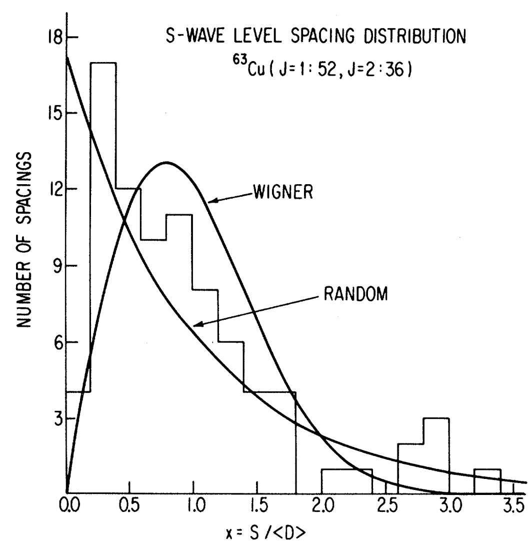


FIG. 7. $S$-wave level spacing distribution for $^{63}$Cu, and its comparison with the theoretical distributions.

spacings in terms of $\Delta_3$ statistics of Dyson and Mehta; however, it is not obvious that this would provide a better handle on the proper assignments of spins of resonances than the reliance on the $R$-matrix fit of the resonances.

### C. Strength functions

The strength function for $l$-wave interaction is calculated from the experimentally determined neutron widths as follows:

$$S_l = \sum_{i=1}^{N} g\Gamma_{ni}^l/(2l+1)\Delta E,$$

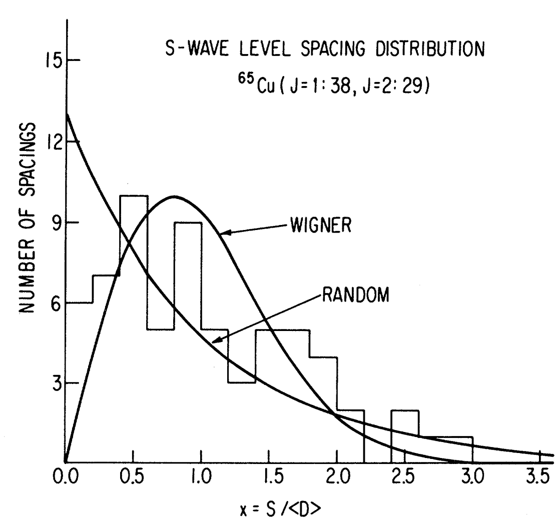


FIG. 8. $S$-wave level spacing distribution for $^{65}$Cu and its comparison with the theoretical distributions.

where $N$ is the number of resonances of angular momentum $l$ observed in the experimental energy range $\Delta E$, $g$ is the spin statistical weight, $\Gamma_n^l$ is the reduced neutron width of angular momentum $l$ and is expressed as

$$\Gamma_{ni}^l = \frac{\Gamma_{ni}}{\sqrt{E_{0i}}} \frac{1}{P_l(k_0 a)},$$

where $k_0$ is the neutron wave number at resonance energy, $a$ is the nuclear radius, and $P_l$ is the penetration factor for angular momentum $l$.

The uncertainty in the determination of the experimental strength function arises from two independent sources, one resulting from the uncertainty in the determination of $\sum g\Gamma_n^l$ (say $\Delta_1$), and the other from the finite number of resonances. The finite sampling error ($\Delta_2$) is estimated as (assuming that the level spacings obey the Wigner distribution)

$$\Delta_2 = \left(\frac{2}{N}\right)^{1/2} S_l ,$$

where $S_l$ is the experimentally determined value of the strength function. The total uncertainty in the strength function is folded as follows:

$$\Delta S_l = \pm(\Delta_1{}^2 + \Delta_2{}^2)^{1/2}.$$

The contribution from $\Delta_1$ is usually much smaller than from $\Delta_2$.

As we have been able to make proper spin assignments to most of the $s$-wave resonances for each nucleus, it was possible to make a determination of the $s$-wave strength function separately for spins $J=1$ and $J=2$. For $p$-wave resonances the strength function is obtained as an average over all possible spins, since it was not possible to make spin determinations for $l=1$ resonances.

A cumulative sum of $\sum\Gamma_n^0$ values as a function of neutron energy was plotted in order to see if there is any evidence of intermediate structure or local fluctuation in the strength function values. For $^{65}$Cu ($J=1$) there was found a clear break in the $\sum\Gamma_n^0$ near about 70–80 keV neutron energy. For $^{63}$Cu the break was less pronounced. We have calculated $S_0$ values from the slopes of the $\sum\Gamma_n^0$ vs $E_n$ curves for two separate energy regions, 10–70 keV and 70–140 keV, respectively. The strength function values for $s$-wave resonances in the different energy intervals as obtained from these measurements are given in Table IX.

The values of the $p$-wave strength function as obtained from these measurements are:

$$^{63}\text{Cu:} \quad S_1 = (0.37 \pm 0.08) \times 10^{-4}\ \text{eV}^{-1/2},$$

$$^{65}\text{Cu:} \quad S_1 = (0.28 \pm 0.06) \times 10^{-4}\ \text{eV}^{-1/2}.$$

A value for nuclear radius of 6 fm was used to calculate $\Gamma_n^1$.

TABLE IX. $S$-wave strength function values (in units of $10^{-4}$) for different energy intervals and for separate spins of $^{63}$Cu and $^{65}$Cu. $R=6\times10^{-13}$ cm.

| Spin state | Energy range (keV) 10–70 | 70–140 | 10–140 | 35–153 [a] |
|---|---|---|---|---|
| | | $^{63}$Cu | | |
| $J=1$ | 3.77±0.80 | 2.17±0.70 | 2.98±0.56 | 1.80±0.52 |
| $J=2$ | 1.03±0.42 | 2.79±0.80 | 2.04±0.46 | 1.78±0.43 |
| $J=1,2$ | 2.40±0.50 | 2.48±0.52 | 2.51±0.37 | 1.80±0.37 |
| | | $^{65}$Cu | | |
| $J=1$ | 2.58±0.88 | 3.10±0.75 | 2.87±0.64 | 1.90±0.54 |
| $J=2$ | 1.12±0.43 | 2.34±0.55 | 1.79±0.49 | 1.22±0.36 |
| $J=1,2$ | 1.85±0.48 | 2.72±0.65 | 2.33±0.38 | 1.51±0.31 |

[a] Reference 8.

These values of $p$-wave strength functions are somewhat smaller than those obtained from the capture measurements; i.e., $S_1=0.44\times10^{-4}$ and $0.47\times10^{-4}$ for $^{63}$Cu and $^{65}$Cu, respectively. This may be due to the fact that we might have missed weak $p$-wave levels in the transmission measurements. For these reasons we have tried to fit the capture values of $S_1$ strength functions with our optical model calculations. The values of the $s$-wave strength function from 10–70 keV for $^{63}$Cu is in good agreement with the values obtained from Columbia measurements[9] up to 50 keV and those obtained by Alves *et al.*[7] up to 30 keV. For $^{65}$Cu, the value of 1.85 obtained in the present result is 50% larger than those obtained both in the Columbia measurement and in the measurement of Alves *et al.*

The comparison of strength functions at the higher energy is made with the results of Beer *et al.*[8] Our results of spin-averaged $S_0$ values both for $^{65}$Cu and $^{63}$Cu in the energy range of 10–140 keV are larger than those obtained by Beer *et al.* Similarly, the values of the strength function for separate spins are in disagreement with the results of Beer *et al.* (See Table IX for a comparison.)

Using the optical model code ABACUS, an attempt was made to reproduce the experimentally determined values of the strength functions by a systematic variation of the optical model parameters. This is done in order to determine the optical model parameters which are consistent with the experimental results, and to provide useful information about the extent of sensitivity of the various parameters on the values of the strength function. The optical model potential used for these calculations has the following form:

$$U_L(r) = -V_L f(r) - iW_L g(r) - V_{so} h(r)(\vec{l}\cdot\vec{\sigma}),$$

where

$$f(r) - \left[1+\exp\left(\frac{r-R}{a_s}\right)\right]^{-1},$$

$$g(r) = -4a_D\frac{d}{dr}\left[1+\exp\left(\frac{r-R}{a_D}\right)\right]^{-1},$$

$$h(r) = -\lambda_\pi^2\frac{1}{r}\frac{d}{dr}\left[1+\exp\left(\frac{r-R}{a_{so}}\right)\right]^{-1},$$

$$R = r_0 A^{1/3}.$$

The values of $r_0$ for the real and imaginary part can be also varied separately in the program.

To obtain a good agreement with the observed results for $^{63}$Cu, the optical model parameters were varied until one obtained the values of $S_0$ and $S_1$ as $S_0 = 2.9\times10^{-4}$ and $S_1 = 0.41\times10^{-4}$. The optical parameters corresponding to these values were ($E_{1ab}$ = 0.06 MeV):

| | | |
|---|---|---|
| $V_{1ab} = 46$ MeV | $r_0 = 1.40$ | $a_s = 0.62$ fm |
| $W_{1ab} = 3.2$ MeV | $r_0 = 1.35$ | $a_D = 0.42$ fm |
| $V_{so} = 7.5$ MeV | $r_0 = 1.35$ | $a_{so} = 0.65$ fm. |

With the same values of the optical parameters, the following values of the strength function were obtained for $^{65}$Cu: $S_0 = 2.1\times10^{-4}$ and $S_1 = 0.48\times10^{-4}$.

These values are within the range of the uncertainty of the experimentally determined values of the strength function. The measured values of $p$-wave strength function for nuclei near $A = 50$ by Stieglitz, Hockenbury, and Block[15] are an order of magnitude smaller than the ones measured in the present work for $A = 63$ and 65. Hence it appears that there still exist large discrepancies in the values of $s$- and $p$-wave strength functions between different measurements. We feel that in view of our superior energy resolution, our values may be more accurate than the previous results of other investigators.

### D. Level density

In the past, values of a large number of experimental energy level spacing near the neutron binding energy have been obtained from neutron total cross section measurements, and these results have been useful in the understanding of the nuclear structure such as the shell and collective effects of nuclear motion.

The total level density $\rho(U)$ is related to the average level spacing $\langle D\rangle$ by the relation $\rho(U) = 1/\langle D\rangle$, and the level density for a given $J$ is given as[16,17]

$$\rho_{(J)} \sim \rho(0)(2J+1)\exp[-(J+\tfrac{1}{2})^2/2\sigma^2], \quad (1)$$

where $\sigma$ is the spin cutoff factor, whose value depends on the particular model and the moment of inertia of the nucleus.

The above expression implies a $(2J+1)$ spin dependence of the level density for $\sigma \gg J$, i.e., one should expect more resonances for higher spin states than for lower spin states. From the present measurement we have obtained the following values for the average level spacings:

$^{63}$Cu $J=1$ $\langle D\rangle = \frac{140}{51} = (2.7\pm0.3)$ keV

$J=2$ $\langle D\rangle = \frac{140}{35} = (4.0\pm0.5)$ keV

$J=1,2$ $\langle D\rangle = (1.63\pm0.13)$ keV

$^{65}$Cu $J=1$ $\langle D\rangle = \frac{140}{38} = (3.7\pm0.4)$ keV

$J=2$ $\langle D\rangle = \frac{140}{28} = (5.0\pm0.7)$ keV

$J=1,2$ $\langle D\rangle = (2.12\pm0.19)$ keV.

Hence both for $^{63}$Cu and $^{65}$Cu the value of the level density is smaller for higher spin ($J=2$) than for lower spin ($J=1$), contrary to what is expected from the theory. The present results of level density are also in disagreement with the results of Beer *et al.*,[8] where they find a larger level density for $J=2$ than for $J=1$ for $^{63}$Cu and about equal values for the two spins for $^{65}$Cu. The variance of the average spacings for $n$ levels observed in a small energy interval for even target nucleus is: $\text{Var}D = 0.27(D^2/n)$. For an odd target nucleus for which there are two possible spins the variance is twice as large when the spin assignments are not made, i.e.,

$$\text{Var}D = 0.54(D^2/n),$$

and the quoted uncertainty is $(\text{Var}D)^{1/2} = (0.54/n)^{1/2}\langle D\rangle$.

In the energy region from 10 to 100 keV we have observed about 57 levels in $^{63}$Cu assigned as $p$ wave, giving a value of mean spacing $\langle D\rangle_{l=1} = \frac{90}{57} = (1.58\pm0.15)$ keV. The average $p$-wave level spacing for $^{65}$Cu is $\frac{90}{49} = (1.84\pm0.19)$ keV. These values are much larger than those obtained in the following paper on capture measurements. This indicates that we have missed many $p$-wave resonances in the transmission or else many resonances observed in the capture measurements should have been assigned as $d$ wave.

For the values of the mean $s$-wave level spacings obtained for individual spin states of copper in the present measurements, we have attempted to evaluate the value of the spin cutoff factor $\sigma$ using relation (1). For the level density ratio ($R = 0.685 \pm^{0.183}_{0.140}$) for ($J=2/J=1$) levels for $^{63}$Cu, one obtained a value of $\sigma = 1.50\pm^{0.25}_{0.16}$. This value of $\sigma$ is much smaller than the value obtained (~3.5) from other measurements. However, the value of $\sigma$ is predicted to vary widely as a function of mass due to shell and other nuclear effects. The present value of $\sigma$ is, however, in agreement with the value of $\sigma = 1.26$, obtained by Green and Hubbard[18] from the MeV energy neutron inelastic, $(n,p)$, and $(n,\alpha)$ cross section measurements in $^{54}Fe$ and $^{58}Fe$. The quoted uncertainty in the value of $\sigma$ is related to the uncertainty in the value of $\langle D\rangle$ for each spin state and does not take into account the factors discussed below.

The values of average level spacings that are obtained from the neutron total cross section data are subject to many uncertainties. This is in part due to Porter-Thomas fluctuation of the neutron widths, which predicts a large probability for small widths. The preponderance of these small widths makes it unlikely to detect almost all the resonances in a given energy interval even with the highest energy resolution. In addition it makes it almost impossible to determine the $l$ and $J$ assignment of such weak resonances with absolute certainty. However, when one determines average values of $D$, the fact that some weak $s$-wave levels may have been missed and some $p$-wave levels have probably been assigned as $s$ wave would help provide a valid value for the $\langle D\rangle$ for $s$-wave levels. Thus, present experimental results appear to be in disagreement with the expected value for $\sigma$ of 3.5 in this mass region. For the case of $p$-wave resonances, the level spacings value is less accurate, since many $p$-wave resonances have not been observed in the total cross section measurements. A discussion of $p$-wave resonances observed in the capture measurements is given in the following paper.

## ACKNOWLEDGMENTS

We would like to thank N. W. Hill for his help in the instrumentation of the experimental setup and for his help in taking the data. Thanks are due to the ORELA operating staff for their cooperation. Thanks are also due to Frank Brown, Wayne Van Pelt, and Jack Craven for their help in the computational analysis. Finally, helpful discussions with Professor Norbert Rosenzweig (SUNYA) are gratefully acknowledged.

---

*Research sponsored by the U.S. Energy Research and Development Administration under contract with Union Carbide Corporation.

†Part of the Ph.D. thesis submitted to the State University of New York at Albany. (Present address: College of William and Mary, Virginia.)

‡Partial travel support provided by the Oak Ridge Associated Universities.

[1]N. A. Betz, J. W. Reynolds, and G. G. Slaughter, in *Proceedings of the Conference on Computer Systems in Experimental Nuclear Physics*, Skytop, Pennsylvania, 2 March 1969 [Columbia University Report No. CONF-69030, 1969) (unpublished)].

[2]N. W. Hill, J. A. Harvey, G. S. Slaughter, and A. St. James, Bull. Am. Phys. Soc. 17, 901 (1972) [also in ORNL-Physics Division Annual Progress Report 1971, No. ORNL-4743].

[3]S. E. Atta and J. A. Harvey, Report No. ORNL 3205, 1961 (unpublished), and addendum 1963.

[4]E. P. Wigner and L. Eisenbud, Phys. Rev. 116, 372 (1947); J. B. Garg, J. Rainwater, and W. W. Havens, Jr., Phys. Rev. C 3, 2447 (1971).

[5]W. M. Good, D. Paya, R. Wagner, and T. Tamura, Phys. Rev. 151, 912 (1966).

[6]H. Marshak and H. W. Newson, Phys. Rev. 106, 110 (1957).

[7]R. N. Alves *et al*., Nucl. Phys. A134, 118 (1969).

[8]H. Beer, R. R. Spencer, and G. Rohr (private communication); Report No. KFK-2056, Karlsruhe, Germany.

[9]J. B. Garg, J. Rainwater, and W. W. Havens, Jr., Report No. CR1860, 1964 (unpublished); M. S. Pandey and J. B. Garg, Nucl. Sci. Eng. (to be published).

[10]*Neutron cross sections,* Brookhaven National Laboratory Report No. BNL-325 (U.S. GPO, Washington, D.C., 1958), 2nd. ed.; Neutron cross sections compiled by M. D. Goldberg *et al*., BNL-325 (National Technical Information Service, Virginia, 1966), 2nd ed., 2nd suppl., Vol. IIA.

[11]M. S. Pandey, J. B. Garg, J. A. Harvey, and W. M. Good, in Proceedings of the International Conference on Nuclear Cross Sections and Technology, March 3–7, 1975, Washington, D.C. (unpublished), p. 748.

[12]C. E. Porter and R. G. Thomas, Phys. Rev. 104, 483 (1956).

[13]E. P. Wigner, in Proceedings of the International Conference on Neutron Interactions with the Nucleus, Columbia University, 9–13 September 1957, edited by W. W. Havens, Jr. [U.S. AEC Report No. TID-1547 (unpublished)].

[14]M. S. Pandey, J. B. Garg, R. L. Macklin, and J. Halperin, following paper, Phys. Rev. C 15, 615 (1977).

[15]R. G. Stieglitz, R. W. Hockenbury, and R. C. Block, Nucl. Phys. A163, 592 (1971).

[16]H. A. Bethe, Rev. Mod. Phys. 9, 84 (1937).

[17]C. Bloch, Phys. Rev. 93, 1094 (1954).

[18]J. M. Green and H. M. Hubbard, in *Proceedings of the International Conference on Statistical Properties of Nuclei*, Albany, August 23–27, 1971, edited by J. B. Garg (Plenum, New York, 1971), p. 663, paper 6.10.